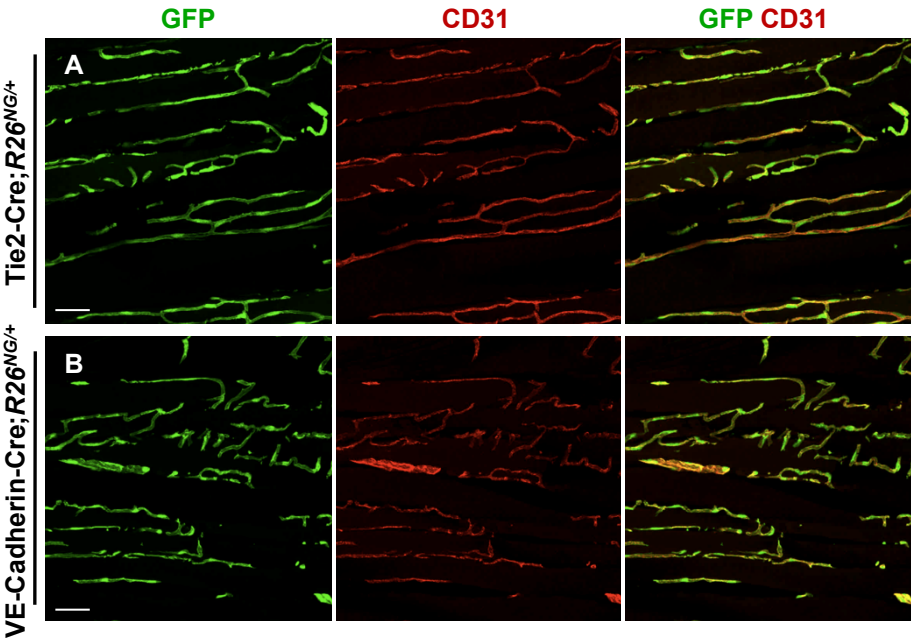
GFP
CD31
GFP CD31
A
Tie2-Cre;R26NG/+
B
VE-Cadherin-Cre;R26NG/+

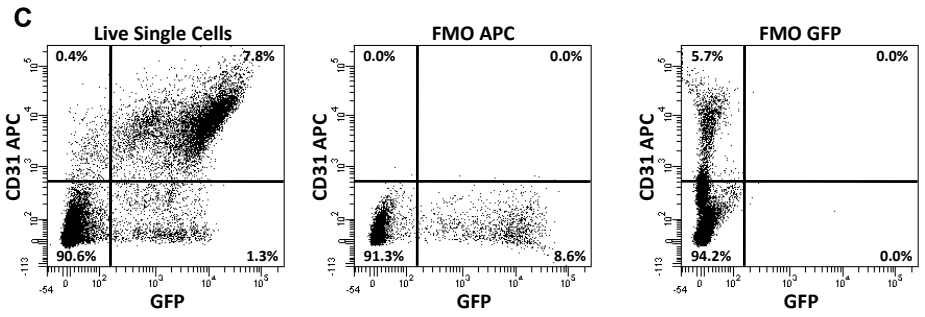
C
Live Single Cells
FMO APC
FMO GFP
CD31 APC
GFP
0.4%
7.8%
90.6%
1.3%
0.0%
0.0%
91.3%
8.6%
5.7%
0.0%
94.2%
0.0%

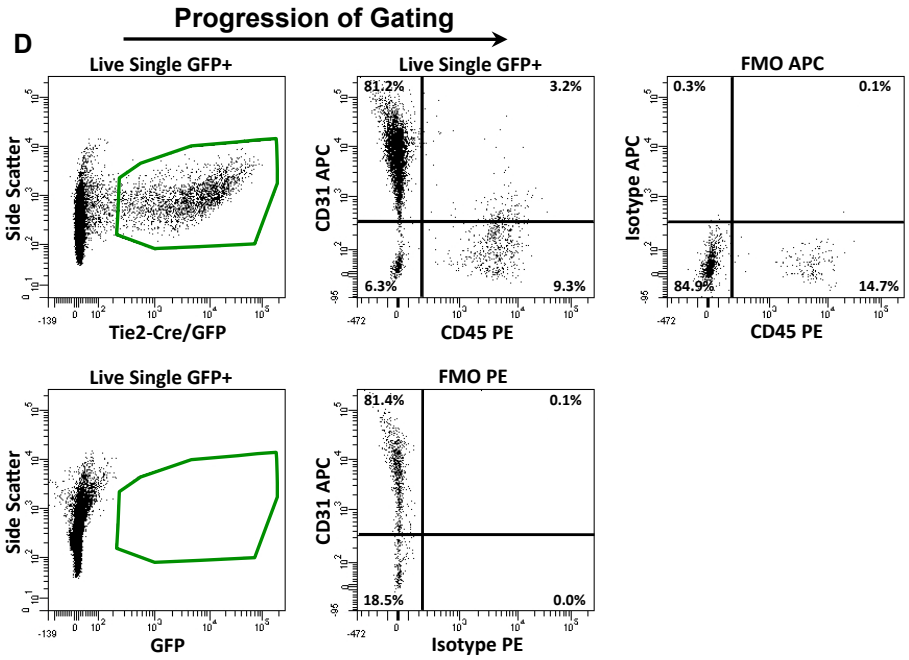
Progression of Gating
D
Live Single GFP+
FMO APC
FMO PE
Side Scatter
Tie2-Cre/GFP
CD31 APC
CD45 PE
Isotype APC
Isotype PE
GFP
81.2%
3.2%
6.3%
9.3%
0.3%
0.1%
84.9%
14.7%
81.4%
0.1%
18.5%
0.0%

Figure S1

Figure S1. Efficient Cre-dependent labeling of the endothelium in Tie2-Cre and VE-Cadherin-Cre transgenic mice. (**A, B**) Longitudinal sections of TA muscles from Tie2-Cre;*R26*$^{NG/+}$ (A) and VE-Cadherin-Cre;*R26*$^{NG/+}$ (B) mice immunostained for the pan-endothelial marker, CD31. All endothelial cells in these views are GFP+. Muscle fibers are not apparent at this exposure. Images are representative of a minimum of three mice for each transgenic line. Scale bars are 40μm. (**C**) GFP+, Cre-recombined cells isolated from total hindlimb muscles of a Tie2-Cre;*R26*$^{NG/+}$ mouse predominantly label endothelium (GFP+CD31+) and, to a lesser extent, an undefined (GFP+CD31-) cell fraction. ~95% of CD31+ cells were GFP+. (**D**) GFP+CD31- cells from a Tie2-Cre;*R26*$^{NG/+}$ mouse can be further fractioned into CD45+ (hematopoietic) and CD45- (undefined) populations.

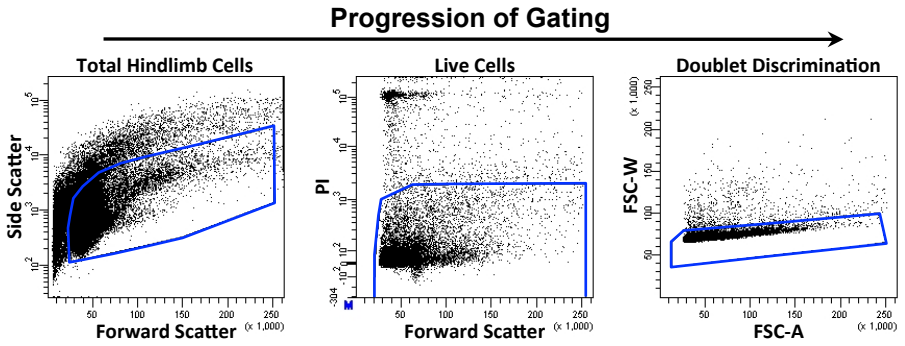
Progression of Gating
Total Hindlimb Cells
Side Scatter
Forward Scatter
(x 1,000)
Live Cells
PI
Forward Scatter
(x 1,000)
Doublet Discrimination
FSC-W
FSC-A
(x 1,000)

Figure S2

Figure S2. Early sorting parameters established to isolate viable cells. Gates were applied to forward/side scatter, live/dead and doublet discrimination FACS plots to exclude debris, dead cells and cell aggregates, respectively. Plots are representative of gating strategies for all cell analyses and sorting data presented.

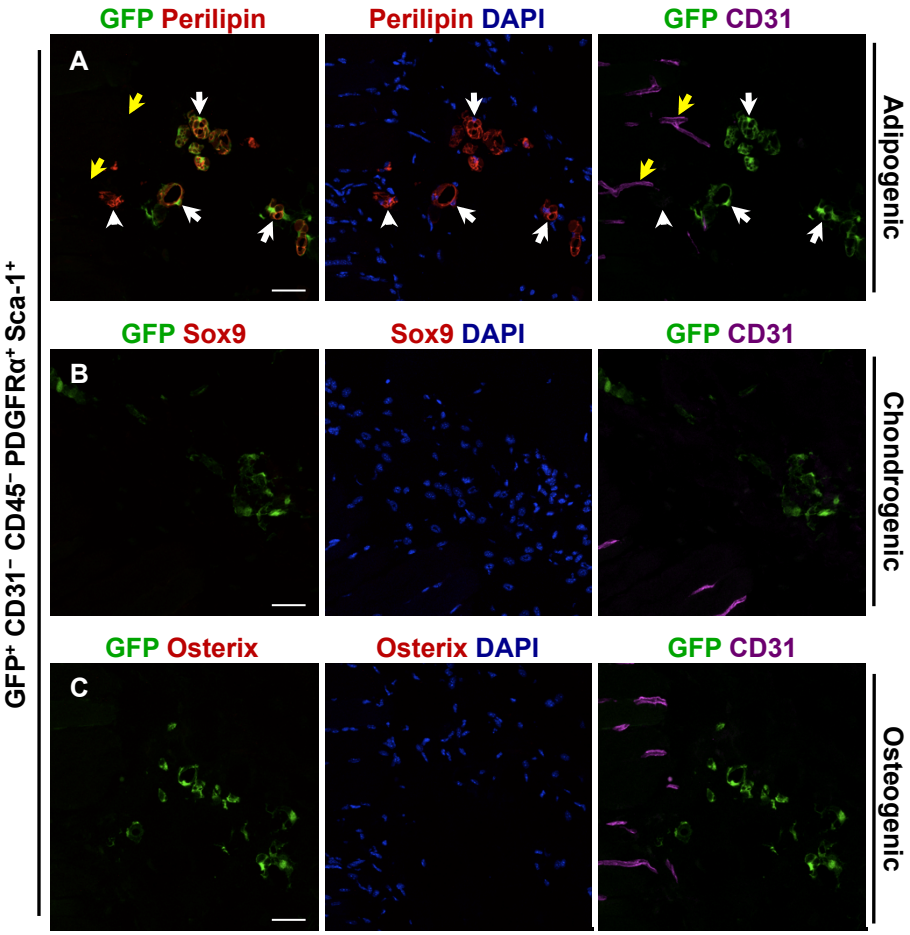
GFP Perilipin
Perilipin DAPI
GFP CD31
A
Adipogenic
GFP Sox9
Sox9 DAPI
GFP CD31
B
Chondrogenic
GFP Osterix
Osterix DAPI
GFP CD31
C
Osteogenic
GFP+ CD31− CD45− PDGFRα+ Sca-1+

Figure S3

Figure S3. GFP+CD31-CD45-PDGFRα+Sca-1+ progenitor cells exhibit BMP2-dependent skeletogenic differentiation and BMP2-independent adipogenic differentiation following intramuscular cell transplantation. (**A-B**) Immunofluorescence images of the TA muscle 10.5d after cell transplantation of cells in Matrigel without the addition of BMP2. (**A**) Transplanted cells contribute to Perilipin+ adipogenic cells (white arrows) but not to CD31+ endothelium (yellow arrows). Adipogenic cells of host origin were also observed (arrowhead). (**B, C**) In the absence BMP2, neither the transplanted cells (GFP+) nor the host (GFP-) were chondrogenic (B) or osteogenic (C). Sections of BMP2-induced lesions were stained in parallel to verify Osterix and Sox9 reactivity. Scale bars are 40μm.

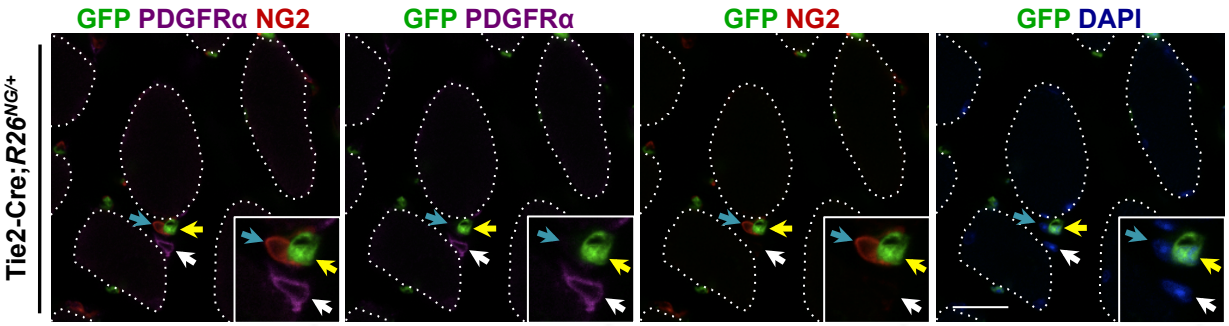

Figure S4

Figure S4. Pericytes and muscle-derived PDGFRα+ cells are distinct. Confocal immunofluorescence images of a cross section of the Soleus muscle from a Tie2-Cre;*R26*$^{NG/+}$ mouse. This section was stained for PDGFRα and the pericyte marker, NG2. Dotted lines represent muscle fiber borders. This view shows an NG2+ cell (blue arrows) in close proximity to both a GFP+ presumptive endothelial cell (yellow arrows) and a PDGFRα+ cell that is negative for GFP (white arrows; presumptive progenitor—see Fig. 6 and Supplemental Figs. S4 and S5). Note that NG2 and PDGFRa are not co-expressed. Scale bar is 20μm.

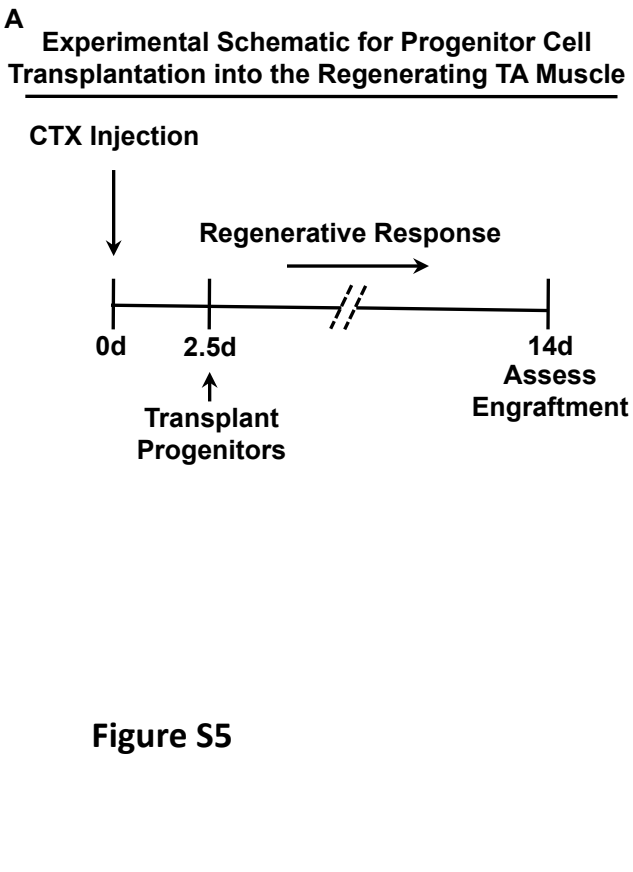
A
Experimental Schematic for Progenitor Cell Transplantation into the Regenerating TA Muscle
CTX Injection
Regenerative Response
0d
2.5d
14d
Assess Engraftment
Transplant Progenitors
B
Post-Injury Engraftment
Laminin DAPI
GFP Laminin DAPI

Figure S5

Figure S5. Transplanted GFP+CD31-CD45-PDGFRα+Sca-1+ progenitor cells occupy the interstitial space of regenerating muscle of SCID mice and do not contribute to nascent muscle fibers. (**A**) Experimental outline. (**B**) Representative confocal images of a TA muscle transverse section 14 days after cardiotoxin (CTX)-induced injury showing the location of transplanted progenitor cells. Note the interstitial location of the engrafted progenitors (white arrows) relative to regenerating muscle fibers (centrally-localized nuclei, yellow arrows), which are circumscribed by Laminin+ basal laminae. No GFP+ muscle fibers were observed in two independent experiments. Scale bar is 20μm.

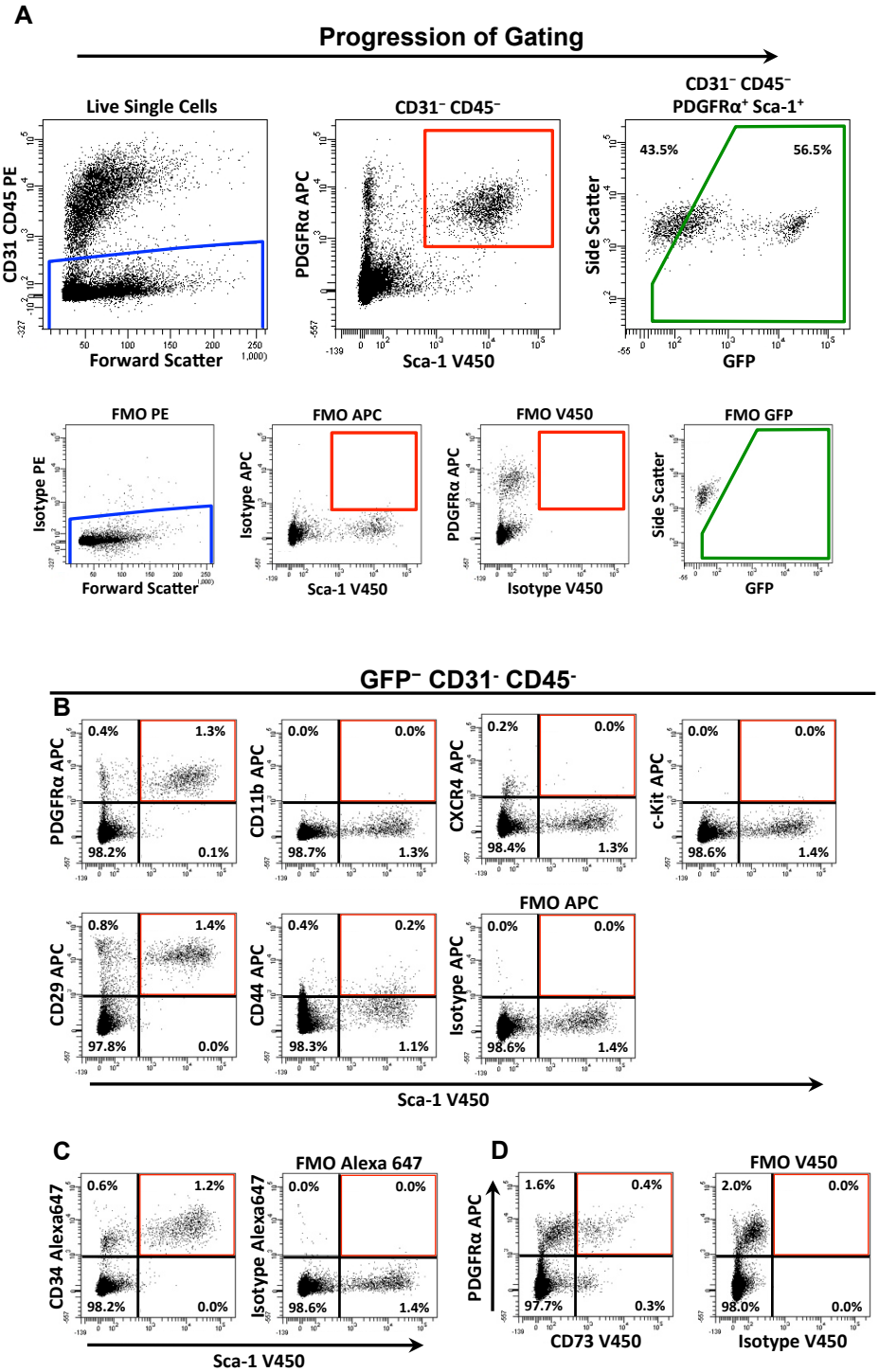
A
Progression of Gating
Live Single Cells
CD31 CD45 PE
Forward Scatter
CD31⁻ CD45⁻
PDGFRα APC
Sca-1 V450
CD31⁻ CD45⁻
PDGFRα⁺ Sca-1⁺
43.5%
56.5%
Side Scatter
GFP
FMO PE
Isotype PE
Forward Scatter
FMO APC
Isotype APC
Sca-1 V450
FMO V450
PDGFRα APC
Isotype V450
FMO GFP
Side Scatter
GFP
GFP⁻ CD31⁻ CD45⁻
B
PDGFRα APC
0.4%
1.3%
98.2%
0.1%
CD11b APC
0.0%
0.0%
98.7%
1.3%
CXCR4 APC
0.2%
0.0%
98.4%
1.3%
c-Kit APC
0.0%
0.0%
98.6%
1.4%
CD29 APC
0.8%
1.4%
97.8%
0.0%
CD44 APC
0.4%
0.2%
98.3%
1.1%
FMO APC
Isotype APC
0.0%
0.0%
98.6%
1.4%
Sca-1 V450
C
CD34 Alexa647
0.6%
1.2%
98.2%
0.0%
FMO Alexa 647
Isotype Alexa647
0.0%
0.0%
98.6%
1.4%
Sca-1 V450
D
PDGFRα APC
1.6%
0.4%
97.7%
0.3%
CD73 V450
FMO V450
2.0%
0.0%
98.0%
0.0%
Isotype V450

Figure S6

Figure S6. FACS characterization of the GFP-CD31-CD45-PDGFRα+Sca-1+ progenitors derived from Tie2-Cre;*R26*$^{NG/+}$ skeletal muscle. (**A**) GFP+ and GFP- cells represent approximately 56% and 44%, respectively, of the CD31-CD45-PDGFRα+Sca-1+ population. Analysis gates were based on FMOs, as shown. (**B-D**) Cell surface antigen profiling of the GFP-CD31-CD45-Sca-1+PDGFRα+ population. The analysis was similar to that of the GFP+ population in Fig. 4. The GFP+ and GFP- subfractions of the CD31-CD45-PDGFRα+Sca-1+ population display similar marker profiles. Note, however, the broader ranges of Sca-1 and CD34 expression levels compared to the GFP+ fraction (Fig. 4), suggesting greater heterogeneity among the GFP-CD31-CD45-PDGFRα+Sca-1+ cell population.

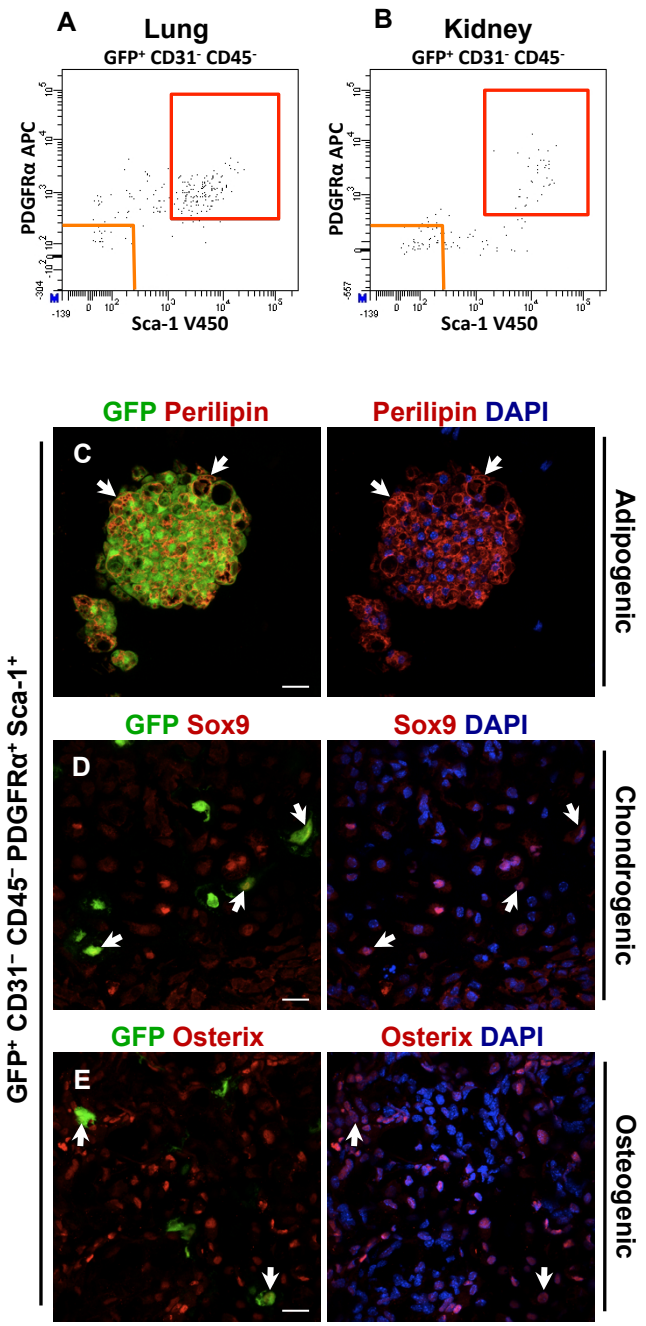
A
Lung
GFP+ CD31- CD45-
PDGFRα APC
Sca-1 V450
B
Kidney
GFP+ CD31- CD45-
PDGFRα APC
Sca-1 V450
GFP+ CD31− CD45− PDGFRα+ Sca-1+
GFP Perilipin
Perilipin DAPI
C
Adipogenic
GFP Sox9
Sox9 DAPI
D
Chondrogenic
GFP Osterix
Osterix DAPI
E
Osteogenic

Figure S7

Figure S7. Identification of GFP+CD31-CD45-PDGFRα+Sca-1+ progenitor cells in lung and kidney. (**A, B**) FACS analysis reveals the presence of GFP+CD31-CD45-PDGFRα+Sca-1+ progenitor cells in the lung (A, red gate) and kidney (B, red gate). Gates (red and orange boxes) were based on FMOs and are similar to the ones used for hindlimb muscle fractionations. (**C-E**) 3.7 X 10^3 GFP+CD31-CD45-PDGFRα+Sca-1+ kidney-derived cells from Tie2-Cre;$R26^{NG/+}$ mice, the total yield from four kidneys, were tested for BMP2-dependent osteogenic activity following intramuscular transplantation into SCID mice. Cryostat sections of 10.5d lesions were stained for Perilipin (C), Sox9 (D) and Osterix (E) to assess adipogenic, chondrogenic and osteogenic differentiation, respectively. Kidney-derived progenitors had similar potencies to those of muscle-derived progenitors, contributing to adipocytes (C), chondrocytes (D) and osteocytes/osteoblasts (E) of the BMP2-induced skeletal anlagen (examples at white arrows). Progenitor cell engraftment was low compared to results obtained with muscle-derived progenitors, probably due to the smaller number of cells injected. Scale bars are 20μm.

Supplemental Table. Antibodies used in experiments

Primary Antibody FACS	Conjugate	Dilution	Clone	Company
CD11b	APC	1:400	M1/70	Ebioscience
CD29	APC	1:400	HMb1-1	Ebioscience
CD31	APC, PE	1:750	390,390	Ebioscience
CD34	Alexa Fluor 647	1:50	RAM34	BD Pharmingen
CD44	APC	1:400	1M7	Ebioscience
CD45	PE	1:800	30-F11	Ebioscience
CD73	V450	1:100	TY/11.8	Ebioscience
CD117 (c-Kit)	APC	1:100	2B8	Ebioscience
CD184 (CXCR4)	APC	1:100	2B11	Ebioscience
PDGFRα	APC	1:50	APA5	Ebioscience
Sca-1	V-450	1:400	D7	BD Pharmingen
Primary Antibody Immunofluorescence	**Conjugate**	**Dilution**	**Clone**	**Company**
CD31	Unconjugated	1:100	MEC13.3	BD Pharmingen
Laminin	Unconjugated	1:600	Polyclonal	Sigma
NG2	Unconjugated	1:250	Polyclonal	Millipore
Osterix	Unconjugated	1:250	Polyclonal	AbCam
Perilipin	Unconjugated	1:500	Polyclonal	Sigma
PDGFRα	Unconjugated	1:100	Polyclonal	R&D Systems
Sca-1	Unconjugated	1:100	D7	Ebioscience
SMA	Unconjugated	1:350	Polyclonal	AbCam
Sox9	Unconjugated	1:100	Polyclonal	Millipore
UCP1	Unconjugated	1:100	Polyclonal	AbCam
Isotype Control	**Conjugate**	**Dilution**	**Clone**	**Company**
Rat IgG	APC	Same as 1^0 Ab Dilution	eBR2a	Ebioscience
Rat IgG	PE		eBR2a	Ebioscience
Rat IgG	Alexa Fluor 647		R35-95	BD Pharmingen
Rat IgG	V450		R35-95	BD Pharmingen
Secondary Antibody	**Conjugate**	**Dilution**		**Company**
Goat anti-rabbit	Alexa Fluor 568 Alexa Fluor 555 Alexa Fluor 546	1:500 1:500 1:500		Invitrogen
Goat anti-rat	Alexa Fluor 568 Alexa Fluor 546 Alexa Fluor 633	1:500 1:500 1:500		Invitrogen
Donkey anti-rabbit	Alexa Fluor 555	1:500		Invitrogen
Donkey anti-rat	Alexa Fluor 594	1:500		Invitrogen
Donkey anti-goat	Alexa Fluor 633	1:500		Invitrogen
Anti-rabbit	Biotinylated	1:250		BD Pharmingen
Streptavidin	Alexa Fluor 555	1:100		Invitrogen